






MODELING THE EFFECT OF QUARANTINE AND HOSPITALIZATION ON THE SPREAD OF COVID-19 DURING THE TOUGHEST PERIOD OF THE PANDEMIC

A.A. AYOADE  , P.A. IKPECHUKWU , S. THOTA , AND O.J. PETER 

Article type: Research Article

(Received: 19 April 2022, Received in revised form 12 September 2022)

(Accepted: 09 December 2022, Published Online: 09 December 2022)

ABSTRACT. The year 2020 arrives with COVID-19. The pandemic poses a formidable threat to human existence at onset but is fought with various measures of which quarantine and hospitalization play a key role. In this article, a COVID-19 transmission mathematical model is developed to assess how quarantine and hospitalization aid improvement in the recovery of both asymptomatic and symptomatic infectious individuals during the toughest period of the pandemic in the year 2020. The basic properties of the model in terms of positivity and boundedness of solutions are discussed based on some ample mathematics theorems. The control reproductive ratio is derived using the next generation matrix approach and the local and global stabilities are investigated via stability theory of differential equations, which depend on the size of the derived control reproductive ratio. Numerical simulation is performed to confirm the analytical results. Findings from the simulation show that quarantine and hospitalization are helpful in averting imminent destruction posed by the pandemic in the years 2020 and early 2021 by reducing both COVID-19 transmission and mortality.

Keywords: COVID-19, Quarantine, Hospitalization, Model, Reproductive ratio.

2020 MSC: 34D23, 92D30, 92B05.

1. Introduction

December 2019 saw the start of a severe respiratory illness in Wuhan, an 11 million-person city in central China. The coronavirus, which was discovered from one patient in January 2020 and later verified in 16 other cases, was blamed for the sickness [30]. The coronavirus was linked to a zoonotic source. Specifically, a market in Wuhan, the Huanan Seafood Market, where live animals were sold, was implicated as the source of the epidemic, as it was discovered that about 234 out of 425 first confirmed cases were traced to the market [23]. Later, further assessment of the inherent sequences of the virus and coronaviruses of bats indicated a 96% resemblance [10,24]. It was the third

✉ ayoayoade@unilag.edu.ng, ORCID: 0000-0003-3470-0147

DOI: 10.22103/jmmr.2022.19335.1236

Publisher: Shahid Bahonar University of Kerman

How to cite: A.A. Ayoade, P.A. Ikpechukwu, S. Thota, O.J. Peter, *Modeling the Effect of Quarantine and Hospitalization on the Spread of COVID-19 during the Toughest Period of the Pandemic*, J. Mahani Math. Res. 2023; 12(1): 339-361.



© the Authors

human zoonotic coronavirus evolving in the present century, after the 2002 outbreak of severe acute respiratory syndrome coronavirus (SARS-CoV) which spread to 37 nations and the 2012 outbreak of Middle East respiratory syndrome coronavirus (MERS-CoV) that spread to 27 countries [13, 32]. Typical symptoms and signs of COVID-19 illness include fatigue, persistent dry cough, fever, difficulty in breathing, and two-sided infiltration of lung in acute cases, comparable to those triggered by MERS-CoV and SARS-CoV infections [?, 3]. Some infected individuals may also exhibit non-respiratory symptoms and signs like vomiting, nausea and diarrhea [12, 16].

The pandemic is still ravaging the world. The incidence and fatality increased astronomically in the early stage of the pandemic in the year 2020 [14]. Within the first four months of the outbreak before May 2020, more than 3 million cases and 230,000 deaths were attributed to COVID-19 and the outbreak spread to more than 210 countries globally [18]. Like other two coronaviruses (SARS-CoV and MERS-CoV), COVID-19 (SARS-CoV-2) can spread from human-to-human through direct contact with infected surfaces or objects and also, through inhalation of droplet from both asymptomatic and symptomatic infected individuals [26, 33]. However, unlike SARS-CoV that accounted for 8 000 confirmed cases and 744 fatalities within just 29 countries and MERS-CoV which caused 2 519 reported cases and 866 deaths within 27 countries, COVID-19 established exponential potential both in terms of confirmed cases and fatalities within few weeks of outbreak [18]. For instance, the first COVID-19 case was recorded in New York on March 1, 2020 and before the end of March the number of reported cases had increased to about 70 000 with almost 1 000 fatalities. The confirmed cases of COVID-19 in New York City jumped to over 300 000 and the mortality from the infection increased to 17 000 before the end of April 2020 [18]. A good number of COVID-19 related mortalities and acute cases emanated from the elderly (65 years old and above) and individuals with comorbidities (such as individuals with obesity, hypertension, diabetes, kidney disease, and other ailments that weaken the immune system such as individuals who have been infected with HIV) [18]. Frontline healthcare personnel and younger people are also at risk of contracting COVID-19 if they come in contact with the infectious agents.

Many issues complicated the spread of COVID-19 and intensified challenges to the control of the disease when it broke out in December 2019. First and foremost, the source of the disease was unknown, although wild animals such as civets, bats and minks were implicated for the outbreak of the epidemic [32]. Second, clinical evidence confirmed the incubation period of 2 to 14 days for the disease [35]. During the incubation, infected persons might not exhibit any signs or symptoms and might be unaware of their clinical status, yet they could spread the infection to other individuals [28]. Third, the agent of the disease was new and there were no certified vaccines or antiviral drugs to combat the scourge [31]. Consequently, disease management heavily relied on timely recognition and isolation of confirmed cases. Also, efforts directed towards the

mitigation and control of the burden of the disease focused on the application of non-pharmaceutical strategies, such as lockdowns, social distancing, quarantine, using face-masks, isolation, hospitalization, and contact-tracing [18,34].

Many modeling studies have been conducted to gain insight into the dynamics of COVID-19 epidemic. Wu et al. [31] presented a (SEIR) model to analyze the dynamics, and predicted the global and national transmission of the disease, according to the reported data from the end of December 2019 to the end of January 2020. The reproductive ratio for COVID-19 was estimated at 2.68 by the researchers. Read et al. [27] computed 3.1 for the reproductive ratio of COVID-19 from the data fitted to a model, employing Poisson-distributed time increments. Tang et al. [29] formulated a model that incorporated disease progression, epidemiological status of the individuals, and the intervention strategies. They discovered that the effective reproductive ratio could be as outrageous as 6.47, and that control measures such as adequate contact tracing, isolation and quarantine could limit the effective reproductive ratio and the spread of the disease. Imai et al. [21] performed computational modeling to compute the magnitude of COVID-19 outbreak in Wuhan city, with an emphasis on the man-to-man transmission. Their results showed that control strategies must be strong enough to avert at least 60% spread of COVID-19 before the menace of the outbreak could be put into proper control. Zhu et al. [19] formulated an algorithm to examine the infectivity of COVID-19 and forecast its possible hosts. Their results implicated minks and bats as the two potential hosts for the virus. Yang and Wang [32] formulated a model to examine both the environment-to-human and human-to-human transmission pathways of COVID-19. Their results advocated long-term intervention and prevention measures as COVID-19 was capable of remaining endemic for as long as possible. Recent studies on COVID-19 can also be assessed in the literature (see for example, [1, 7, 25]).

Hospitalization and quarantine were crucial tools in the fight against the ongoing coronavirus epidemic that paralyzed the world in 2020. The virus posed a formidable threat to human existence and seemed to have a potential to wipe out the human race from the surface of the earth by its ability to bring the world powers to their knees at onset in the year 2020. However, quarantine and hospitalization brought the hope of defeating COVID-19 and saved man from imminent destruction. The present paper therefore, presents a mathematical model to examine the effect of quarantine and hospitalization on the dynamics of COVID-19 since the model published so far have not exclusively considered the impact of quarantine and hospitalization on the transmission and spread of COVID-19 especially during the toughest period of the pandemic in the year 2020. The study uses a mathematical modeling approach to assess how quarantine and hospitalization aided improvement in the recovery of both asymptomatic and symptomatic infectious individuals during the toughest period of COVID-19 pandemic in the year 2020.

This paper is organised as follows: Section 2 introduces the model formulation and the proofs of some theorems to verify the existence and validity of the model. The analytical solutions of the model in terms of the equilibria, reproductive ratio and stability are obtained in section 3. Numerical simulation is carried out in Section 4 to verify the analytical results obtained in this paper.

2. Model Formulation and Basic Properties

The model is developed on the ground that coronavirus can be spread from human-to-human and from environment-to-human [32]. Besides, since the disease is highly associated with migration, immigration and quarantine are considered and those who arrive from other territories are put in quarantine for two weeks which is the general practice globally. The human population is made up of seven compartments: the susceptible S , the exposed E , the infected I , the quarantined Q , the hospitalized H , the recovered individuals R and the contaminated environment V . If per capita probability of arriving from other territories is π then the proportion $b\pi$ are recruited into the quarantine class for two weeks while the remaining proportion $b(1 - \pi)$ are recruited into the susceptible class at the same rate b . Individuals in the exposed and infected compartments are both infectious while the susceptible individuals can contract the virus from both of them and from the contaminated environment V at rates β_1 , β_2 and β_3 respectively.

Due to the awareness campaigns and other measures like contact tracing, some individuals in the exposed class are detected before they become symptomatic. If per capita probability of being detected at the exposed stage is σ then the proportion $\phi\sigma$ moves to the quarantine class while the remaining proportion $\phi(1 - \sigma)$ moves to the infectious class at the same rate ϕ . Individuals who arrive from other territories that are put in the quarantine class do not interact with the exposed individuals who are also in the quarantine class and as a result, do not pick up the virus. Individuals in the infected class are hospitalized at rate θ while disease-induced mortality occurs for the infected and the hospitalized compartments at rates d_1 and d_2 respectively. After two weeks, individuals who arrive from other territories in the quarantine class either move to the hospitalized class if they test positive to the virus or to the recovered class if they test negative. Those that are tested negative are moved to the recovered class and not to the susceptible class because a policy has been put in place to monitor them from contracting the virus. If per capita probability of being positive is ρ then the proportion $\tau\rho$ moves to the hospitalized class while the remaining proportion $\tau(1 - \rho)$ moves to the recovered class at the same rate τ . Individuals in the hospitalized class clear the virus and move to the recovered class at rate α and every individual who is in the recovered class remains in the class throughout the analysis. Infectious individuals shed pathogens to the environment at rates k_1 and k_2 respectively while the pathogens are removed

from the environment rate ϵ . Natural mortality occurs in all human compartments at rate μ . The movement between the compartments is illustrated in Figure 1

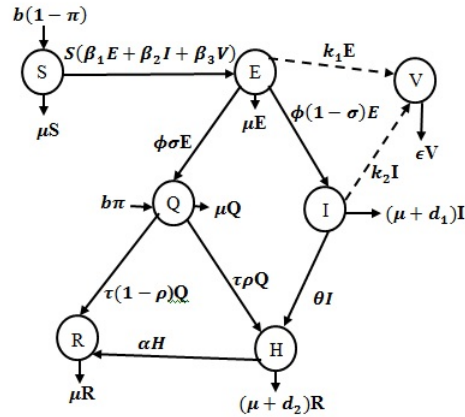


Figure 1: The model transfer diagram

FIGURE 1. Transfer diagram of the model.

In view of the stated assumptions and the transfer diagram, the following set of first-order nonlinear ordinary differential equations are derived.

$$\begin{aligned}
 (1) \quad & \frac{dS}{dt} = b(1 - \pi) - \beta_1SE - \beta_2IS - \beta_3SV - \mu S, \\
 (2) \quad & \frac{dE}{dt} = \beta_1SE + \beta_2IS + \beta_3SV - (\phi + \mu)E, \\
 (3) \quad & \frac{dI}{dt} = \phi(1 - \sigma)E - (\theta + d_1 + \mu)I, \\
 (4) \quad & \frac{dQ}{dt} = b\pi + \phi\sigma E - (\tau + \mu)Q, \\
 (5) \quad & \frac{dH}{dt} = \tau\rho Q + \theta I - (\alpha + d_2 + \mu)H, \\
 (6) \quad & \frac{dR}{dt} = \tau(1 - \rho)Q + \alpha H - \mu R, \\
 (7) \quad & \frac{dV}{dt} = k_1E + k_2I - \epsilon V.
 \end{aligned}$$

The nomenclatures for the parameters are redefined in Table 1 for quick reference.

TABLE 1. Definition of model parameters.

Parameters	Nomenclatures
b	human recruitment rate
π	proportion of individuals who arrived from other territories
β_1	effective contact rate between those who are exposed and those who are susceptible
β_2	effective contact rate between infected people and those who are susceptible
β_3	effective rate of contact between susceptible people and the contaminated environment
μ	natural mortality rate in all human classes
ϕ	progression rate from asymptomatic stage
σ	proportion of individuals who are detected at the asymptomatic stage
θ	hospitalization rate after being fully symptomatic
d_1	mortality rate due to infection at symptomatic stage
d_2	mortality rate due to infection during hospitalization or treatment failure rate
τ	rate of coming out of quarantine
ρ	proportion of individuals who are tested positive to COVID-19 after leaving quarantine
α	treatment success rate or recovery rate
k_1	the rate at which asymptomatic people contribute to the growth of the pathogen
k_2	the rate at which symptomatic individuals contribute to the pathogen's expansion
ϵ	rate of pathogen elimination from the environment

The sum of the components of the model at time t is defined by

$$(8) \quad N(t) = S(t) + E(t) + I(t) + Q(t) + H(t) + R(t) + V(t),$$

with the functions (S, E, I, Q, H, R, V) , defined on $[0, T] : \forall 0 < t \leq T$, the system (1)-(7) holds with the initial conditions

$$(9) \quad S(0) = S_0, E(0) = E_0, I(0) = I_0, Q(0) = Q_0, H(0) = H_0, R(0) = R_0, V(0) = V_0.$$

In Eq.(9), $S_0 > 0$ represents initial human population before disease outbreak while E_0, I_0, Q_0, H_0, R_0 and V_0 are positive initial populations in each compartment. It is obvious that $N(t)$ in Eq.(8) is made up of two compartments, Γ and Ψ , human and pathogen populations respectively such that

$$(10) \quad N(t) = \Gamma + \Psi,$$

where

$$(11) \quad \Gamma = S(t) + E(t) + I(t) + Q(t) + H(t) + R(t),$$

and,

$$(12) \quad \Psi = V(t).$$

At the onset of the epidemic, it is usually assumed that only the susceptible exists such that $S_0 = N(0) > 0$ while other populations disappear. The analysis, however, permits positive initial populations for all the state variables for the purpose of argument such that Eq.(10) is valid at $t = 0$ and $N(0) = S_0 + E_0 + I_0 + Q_0 + H_0 + R_0 + V_0$.

Eq.(1) expresses changes in the population of the susceptible $S(t)$ with time. The second, third and fourth terms on the RHS illustrate the degree at which the individuals in the susceptible compartment contract the virus by interacting with the exposed and the symptomatic infected individuals as well as the contaminated environment. The final term in Eq.(1) denotes the natural death in the susceptible class.

The incubation period for COVID-19 is between 2-14 days [8] and given the natural death rate μ with a life expectancy period of 75 years then, $\mu = 0.000037$ per day. With nonexistence of infection, the total human population in Eq.(11) converges to $\Gamma = \frac{b(1 - \pi)}{\mu} = 3\,000\,000$ (i.e., the value of S at DFE). Hence, the total susceptible individuals in a day is $b(1 - \pi) = 111$. $b(1 - \pi)$ is the recruitment within the population only (i.e through birth). It excludes movement from other territories. The values used for other parameters in the simulation process are displayed in Table 2.

Lastly, the aggregate mortality caused by the infection could be derived from

$$(13) \quad F(t) = \int_0^t (d_1 I(\varphi) + d_2 H(\varphi)) d\varphi,$$

with $F(0) = 0$.

Existence, Boundedness and Positivity of Solutions. The solutions of the model are analyzed for the existence, positivity and boundedness properties which are based on the usual considerations for ODEs, given that the RHS of the model (1)-(7) is Lipschitz continuous. Subsequently, to establish the validity of the model biologically, the nonnegativity properties of the model solutions must be established.

Theorem 2.1. *Assuming the initial populations meet the requirement $S(0) > 0$, $E(0) \geq 0$, $I(0) \geq 0$, $Q(0) \geq 0$, $H(0) \geq 0$, $R(0) \geq 0$ and $V(0) \geq 0$. Therefore, the solutions $(S(t), E(t), I(t), Q(t), H(t), R(t), V(t))$ of the system are positive and bounded on the interval $[0, T]$ where the solutions exist.*

Proof. Let $0 < t < T$ and represent by λ , the aggregate force of infection, i.e.,

$$(14) \quad \lambda = \beta_1 E + \beta_2 I + \beta_3 V,$$

where Eq.(10) is valid, i.e.,

$$N = S + E + I + Q + H + R + V.$$

It suffices from Eq.(1) that

$$(15) \quad \begin{aligned} \frac{dS}{dt} &= b(1 - \pi) - \lambda S - \mu S, \\ &\geq -(\lambda + \mu)S. \end{aligned}$$

Following variable separable method and integrating on $[0, t]$, as well as using the initial conditions, Eq.(15) becomes

$$(16) \quad S(t) \geq S(0) \exp \left(- \int_0^t \lambda(s) ds - \mu t \right) \geq 0.$$

Hence, $S(t) > 0$ in Eq.(16) since $S(0) > 0$. Also, in Eq.(2),

$$(17) \quad \frac{dE}{dt} = \lambda S - (\phi + \mu)E,$$

which results in

$$(18) \quad E(t) \geq E(0)e^{-(\phi+\mu)t} \geq 0.$$

Also, in Eqs.(3),(4),(5),(6) and (7), it follows that

$$(19) \quad I(t) \geq I(0)e^{-(\theta+d_1+\mu)t} \geq 0,$$

$$(20) \quad Q(t) \geq Q(0)e^{-(\tau+\mu)t} \geq 0,$$

$$(21) \quad H(t) \geq H(0)e^{-(\alpha+d_1+\mu)t} \geq 0,$$

and

$$(22) \quad R(t) \geq R(0)e^{-\mu t} \geq 0.$$

Finally,

$$(23) \quad \begin{aligned} \frac{dV}{dt} &= k_1 E + k_2 I - \epsilon V, \\ &\geq -\epsilon V. \end{aligned}$$

Hence, $V(t) \geq V(0)e^{-\epsilon t} \geq 0$. Consequently, the solutions are positive.

Next, the solutions' boundedness are established which follow directly from the preceding results that the model solutions are positive. By summing up the human populations in the system and using Eq.(11), the change in the total human population Γ , with time becomes

$$(24) \quad \frac{d\Gamma}{dt} = b - \mu\Gamma - d_1 I - d_2 H.$$

Hence,

$$b - (\mu + d_1 + d_2)\Gamma \leq \frac{d\Gamma}{dt} \leq b - \mu\Gamma.$$

Therefore,

$$\frac{d\Gamma}{dt} + \mu\Gamma \leq b,$$

such that

$$\begin{aligned} \Gamma(t) &\leq b \int_0^t e^{-\mu(t-s)} ds + \Gamma_0 e^{-\mu t}, \\ &\leq \frac{b}{\mu} (1 - e^{-\mu t}) + \Gamma_0 e^{-\mu t}. \end{aligned}$$

It is therefore concluded that $\Gamma(t)$ is nonnegative and bounded for all $0 \leq t < T$. As for the pathogen population, Eq. (7) can be written as

$$\frac{dV}{dt} = (E + I)\Lambda - \epsilon V.$$

Since the population in V is influenced by the exposed and infected individuals E and I . Therefore, it is in order to write

$$\Psi(t) \leq (E + I)\Lambda \int_0^t e^{-\epsilon(t-\omega)} d\omega + \Psi_0 e^{-\epsilon t},$$

where $\Lambda = \min(k_1, k_2)$ and $(E + I) \leq \frac{b}{\mu}$.

$$\begin{aligned} \Rightarrow \Psi(t) &\leq \frac{b\Lambda}{\mu} \int_0^t e^{-\epsilon(t-\omega)} d\omega + \Psi_0 e^{-\epsilon t}, \\ &\leq \frac{b\Lambda}{\epsilon\mu} (1 - e^{-\epsilon t}) + \Psi_0 e^{-\epsilon t}. \end{aligned}$$

Since $N(t) > 0$ and each of the variables S, E, I, Q, H, R and V are positive, it then follows that all the variables are bounded \square

Based on the importance of the proof of Theorem 1, the existence and uniqueness of solutions of the model is therefore stated in the form of a theorem.

Theorem 2.2. *The exclusive solution $(S(t), E(t), I(t), Q(t), H(t), R(t), V(t))$ exists as long as $t \geq 0$. Further, for all $t \geq 0$, the solution persists within the set $\Omega = \left\{ \Gamma = \Gamma \leq \frac{b}{\mu} + \Gamma_0, \Psi = \Psi \leq \frac{b\Lambda}{\epsilon\mu} + \Psi_0, \right\}$ which is not only compact but positively invariant.*

The solutions of the model therefore exist and are unique. The global existence of the solutions therefore follows from the fact that the model is Lipschitz continuous and the model solutions are bounded.

3. Equilibria, Reproduction Number and Stability

It is easy to notice that the system contains two steady states: an infection-free equilibrium and an infection-persistence equilibrium. The stability of both equilibria shall be studied after the reproduction number is derived.

3.1. Reproduction Number and Stability of zero Equilibrium. The infection-free equilibrium exists when $S = S_0 = \frac{b(1-\pi)}{\mu}$ and $E = I = Q = H = R = V = 0$, and is derived by reducing the RHS of the system (1)-(7) to zero. Furthermore, $N = S = S_0$, hence, the system reduces to $\mu S = b(1-\pi)$, which generates $S_0 = \frac{b(1-\pi)}{\mu}$, and other variables vanish.

Let $x = (E, I, V, Q, H, R, S)^T$, then the system (1)-(7) can be expressed as

$$(25) \quad \frac{dx}{dt} = \mathcal{F} - \mathcal{V},$$

where

$$\mathcal{F} = ((\beta_1 E + \beta_2 I + \beta_3 V)S_0, 0, 0, 0, 0, 0, 0)^T,$$

and,

$$\mathcal{V} = \begin{pmatrix} (\phi + \mu)E \\ -\phi(1 - \sigma)E + (\theta + d_1 + \mu)I \\ -b\pi - \phi\sigma E + (\tau + \mu)Q \\ -\tau\rho Q - \theta I + (\alpha + d_2 + \mu)H \\ -\tau(1 - \rho)Q - \alpha H + \mu R \\ -k_1 E - k_2 I + \epsilon V \\ -b(1 - \pi) + (\beta_1 E + \beta_2 I + \beta_3 V)S_0 + \mu S_0 \end{pmatrix}.$$

To obtain the threshold quantity \mathcal{R}_c , the procedure in [15] is followed and the system is restricted to the populations of the infectious agents (E, I, V) only such that

$$(26) \quad \mathcal{F} = \begin{pmatrix} \beta_1 S_0 & \beta_2 S_0 & \beta_3 S_0 \\ 0 & 0 & 0 \\ 0 & 0 & 0 \end{pmatrix},$$

$$(27) \quad \mathcal{V} = \begin{pmatrix} (\phi + \mu) & 0 & 0 \\ -\phi(1 - \sigma) & (\theta + d_1 + \mu) & 0 \\ -k_1 & -k_2 & \epsilon \end{pmatrix}.$$

$$(28) \quad \mathcal{V}^{-1} = \begin{pmatrix} 1 & 0 & 0 \\ \frac{(\phi + \mu)}{\phi(1 - \sigma)} & 1 & 0 \\ \frac{(\phi + \mu)(\theta + d_1 + \mu)}{k_1(\theta + d_1 + \mu) + k_2\phi(1 - \sigma)} & \frac{(\theta + d_1 + \mu)}{k_2} & \frac{1}{\epsilon} \\ \frac{\epsilon(\phi + \mu)(\theta + d_1 + \mu)}{\epsilon(\phi + \mu)(\theta + d_1 + \mu)} & \frac{\epsilon(\theta + d_1 + \mu)}{\epsilon(\theta + d_1 + \mu)} & \frac{1}{\epsilon} \end{pmatrix}.$$

$$FV^{-1} = \begin{pmatrix} \frac{\beta_1 S_0}{p_1} + \frac{\beta_2 \phi(1 - \sigma)S_0}{p_1 p_2} + \frac{k_1 p_2 \beta_3 S_0 + k_2 \phi(1 - \sigma)S_0}{\epsilon p_1 p_2} & \frac{\beta_2 S_0}{p_2} + \frac{k_2 \beta_3 S_0}{\epsilon p_2} & \frac{\beta_3 S_0}{\epsilon} \\ 0 & 0 & 0 \\ 0 & 0 & 0 \end{pmatrix}, \quad (29)$$

where

$$p_1 = \phi + \mu \text{ and } p_2 = \theta + d_1 + \mu.$$

Therefore, the eigenvalues of Eq.(29) are

$$\lambda_1 = \frac{\beta_1 S_0}{p_1} + \frac{\beta_2 \phi(1 - \sigma)S_0}{p_1 p_2} + \frac{k_1 p_2 \beta_3 S_0 + k_2 \phi(1 - \sigma)S_0}{\epsilon p_1 p_2}, \lambda_2 = \lambda_3 = 0.$$

Then, the control threshold parameter is obtained as

$$(30) \quad \mathcal{R}_c = \lambda_1 = \frac{\beta_1 S_0}{p_1} + \frac{\beta_2 \phi(1 - \sigma) S_0}{p_1 p_2} + \frac{k_1 p_2 \beta_3 S_0 + k_2 \phi(1 - \sigma) S_0}{\epsilon p_1 p_2}.$$

It is evident from numerous studies, see for instance, [2, 4, 5] that the reproduction number \mathcal{R}_0 is quantified without control measures, which in the present analysis means $\sigma = 0$ and $\theta = 0$. \mathcal{R}_0 is therefore derived from \mathcal{R}_c when σ and θ are set to zero thus

$$(31) \quad \mathcal{R}_0 = \lambda_1 = \frac{\beta_1 S_0}{(\phi + \mu)} + \frac{\beta_2 \phi S_0}{(\phi + \mu)(d_1 + \mu)} + \frac{k_1 \beta_3 (d_1 + \mu) S_0 + k_2 \phi S_0}{\epsilon(\phi + \mu)(d_1 + \mu)}.$$

\mathcal{R}_0 and \mathcal{R}_c are related in a way that when σ and θ are zero, no asymptomatic individual is quarantined and no symptomatic person is hospitalized, though, as the analysis is locally around the origin, some quarantine and hospitalized individuals were likely to exist initially. The following results for equilibria stability are proposed.

Theorem 3.1. *The infection-free equilibrium of the system is locally asymptotically stable if $\mathcal{R}_c < 1$ but unstable if $\mathcal{R}_c > 1$.*

Proof. The variational matrix $J(\mathcal{D}_0)$ of the system is derived at the infection-free equilibrium, $\mathcal{D}_0 = (S_0, 0, 0, 0, 0, 0, 0)$ as

$$J(\mathcal{D}_0) = \begin{pmatrix} -\mu & -\beta_1 S_0 & -\beta_2 S_0 & 0 & 0 & 0 & -\beta_3 S_0 \\ 0 & -(\phi + \mu) + \beta_1 S_0 & \beta_2 S_0 & 0 & 0 & 0 & 0 \\ 0 & \phi(1 - \sigma) & -(\theta + d_1 + \mu) & 0 & 0 & 0 & 0 \\ 0 & \phi\sigma & 0 & -(\tau + \mu) & 0 & 0 & 0 \\ 0 & 0 & \theta & \tau\rho & -(\alpha + d_2 + \mu) & 0 & 0 \\ 0 & 0 & 0 & \tau(1 - \rho) & \alpha & -\mu & 0 \\ 0 & k_1 & k_2 & 0 & 0 & 0 & -\epsilon \end{pmatrix}. \tag{32}$$

The characteristic equation of Eq.(32) has five nonpositive eigenvalues: $-(\theta + d_1 + \mu)$, $-(\tau + \mu)$, $-\epsilon$ and $-\mu$ (double). The remaining solutions can be obtained from

$$(33) \quad \mathcal{A} = \begin{pmatrix} -(\phi + \mu) + \beta_1 S_0 & \beta_2 S_0 \\ \phi(1 - \sigma) & -(\theta + d_1 + \mu) \end{pmatrix}.$$

In Eq.(33),

$$tr(\mathcal{A}) = -(\phi + 2\mu + \theta + d_1) + \beta_1 S_0,$$

and,

$$det(\mathcal{A}) = (\phi + \mu)(\theta + d_1 + \mu) - \beta_1 S_0(\theta + d_1 + \mu) - \beta_2 \phi(1 - \sigma) S_0.$$

The two solutions are nonpositive if $tr(\mathcal{A}) < 0$ and $det(\mathcal{A}) > 0$. Hence, $\mathcal{R}_c < 1$ and \mathcal{D}_0 is locally asymptotically stable if the conditions $tr(\mathcal{A}) < 0$ and $det(\mathcal{A}) > 0$ are satisfied. If any of the conditions is not fulfilled then one or both eigenvalues in Eq.(33) is/are positive meaning that \mathcal{D}_0 is locally unstable and $\mathcal{R}_c > 1$. □

3.2. Equilibrium and Stability of Nonzero Equilibrium. The infection-persistence equilibrium of the system is denoted by $\mathcal{D}^* = (S^*, E^*, I^*, Q^*, H^*, R^*, V^*)$ such that $\mathcal{D}^* \neq (S_0, 0, 0, 0, 0, 0, 0)$. The RHS of the system (1)-(7) is set to zero and the resulting equations are solved to find where \mathcal{D}^* exists. The coordinates of \mathcal{D}^* are obtained thus

$$(34) \quad S^* = \frac{1}{\mu}[b(1 - \pi) - (\phi + \mu)E^*],$$

$$(35) \quad I^* = \left(\frac{\phi(1 - \sigma)}{\theta + d_1 + \mu} \right) E^*,$$

$$(36) \quad Q^* = \left(\frac{b\pi + \phi\sigma E^*}{\tau + \mu} \right),$$

$$(37) \quad H^* = \left(\frac{\tau\rho Q^* + \theta I^*}{\alpha + d_2 + \mu} \right),$$

$$(38) \quad R^* = \frac{1}{\mu}[\tau(1 - \rho)Q^* + \alpha H^*],$$

$$(39) \quad V^* = \left(\frac{[k_1(\theta + d_1 + \mu) + k_2\phi(1 - \sigma)]E^*}{\epsilon(\theta + d_1 + \mu)} \right)$$

Combining Eqs.(35),(39) and (2) \Rightarrow

$$(40) \quad \beta_1 S^* E^* + \frac{\beta_2 \phi(1 - \sigma) S^* E^*}{(\theta + d_1 + \mu)} + \frac{\beta_3 [k_1(\theta + d_1 + \mu) + k_2 \phi(1 - \sigma)] S^* E^*}{\epsilon(\theta + d_1 + \mu)} - (\phi + \mu) E^* = 0.$$

There exists two roots in Eq.(40), $E^* = 0$ which relate to the infection-free equilibrium \mathcal{D}_0 and

$$(41) \quad S^* = \frac{(\phi + \mu)}{\beta_1 + \frac{\beta_2 \phi(1 - \sigma)}{(\theta + d_1 + \mu)} + \frac{\beta_3 [k_1(\theta + d_1 + \mu) + k_2 \phi(1 - \sigma)]}{\epsilon(\theta + d_1 + \mu)}}.$$

Multiply the numerator and denominator of Eq.(41) by $\frac{S_0}{(\phi + \mu)}$ then

$$(42) \quad S^* = \frac{S_0}{\mathcal{R}_c},$$

$$(43) \quad E^* = \frac{1}{(\phi + \mu)} \left[b(1 - \pi) - \frac{\mu S_0}{\mathcal{R}_c} \right],$$

$$(44) \quad I^* = \frac{\phi(1 - \sigma)}{(\phi + \mu)(\theta + d_1 + \mu)} \left[b(1 - \pi) - \frac{\mu S_0}{\mathcal{R}_c} \right],$$

$$(45) \quad Q^* = \frac{b\pi}{(\tau + \mu)} + \frac{\phi\sigma}{(\phi + \mu)(\tau + \mu)} \left[b(1 - \pi) - \frac{\mu S_0}{\mathcal{R}_c} \right],$$

$$(46) \quad H^* = \left[\frac{\tau\rho N_1 + \theta N_2}{\alpha + d_2 + \mu} \right],$$

$$(47) \quad R^* = \frac{1}{\mu} [\tau(1 - \rho)N_1 + \alpha N_3],$$

$$(48) \quad V^* = \frac{[k_1(\theta + d_1 + \mu) + k_2\phi(1 - \sigma)]}{\epsilon(\phi + \mu)(\theta + d_1 + \mu)} \left[b(1 - \pi) - \frac{\mu S_0}{\mathcal{R}_c} \right],$$

where

$$N_1 = Q^*, N_2 = I^* \text{ and } N_3 = H^*.$$

In view of Eq.(40) and the fact that the analysis is near the origin then

$$(49) \quad \left[\beta_1 S_0 + \frac{\beta_2 \phi(1 - \sigma) S_0}{(\theta + d_1 + \mu)} + \frac{\beta_3 [k_1(\theta + d_1 + \mu) + k_2 \phi(1 - \sigma)] S_0}{\epsilon(\theta + d_1 + \mu)} - (\phi + \mu) \right] E \leq 0,$$

$$(50) \quad (\phi + \mu) \left[\frac{\beta_1 S_0}{(\phi + \mu)} + \frac{\beta_2 \phi(1 - \sigma) S_0}{(\phi + \mu)(\theta + d_1 + \mu)} + \frac{\beta_3 [k_1(\theta + d_1 + \mu) + k_2 \phi(1 - \sigma)] S_0}{\epsilon(\phi + \mu)(\theta + d_1 + \mu)} - 1 \right] E \leq 0,$$

$$(51) \quad \Rightarrow (\phi + \mu)[\mathcal{R}_c - 1]E \leq 0.$$

If $\mathcal{R}_c < 1$ in Eq.(51) then the only equilibrium that exists around the origin is infection-free equilibrium which is not only locally asymptotically stable but globally asymptotically stable. Conversely, if $\mathcal{R}_c \geq 1$ then there exists a unique infection-persistence equilibrium. The stability of the infection-persistence equilibrium shall be considered next.

Theorem 3.2. *The infection-persistence equilibrium $\mathcal{D}^* = (S^*, E^*, I^*, Q^*, H^*, R^*, V^*)$ exists, unique and is locally asymptotically stable in the neighborhood of the infection-free equilibrium \mathcal{D}_0 whenever $\mathcal{R}_c > 1$.*

Proof. Let $S = x_1, E = x_2, I = x_3, Q = x_4, H = x_5, R = x_6, V = x_7$ and denote $\mathbf{x} = (x_1, x_2, x_3, x_4, x_5, x_6, x_7)$ such that

$$N = x_1 + x_2 + x_3 + x_4 + x_5 + x_6 + x_7.$$

The model (1)-(7) is then rewritten as

$$\frac{dx}{dt} = \mathbf{f} = (f_1, f_2, f_3, f_4, f_5, f_6, f_7),$$

with components \mathbf{f} and the model given as

$$(52) \quad \frac{dx_1}{dt} = f_1 = b(1 - \pi) - \beta_1^* x_1 x_2 - \beta_2 x_1 x_3 - \beta_3 x_1 x_7 - \mu x_2,$$

$$(53) \quad \frac{dx_2}{dt} = f_2 = \beta_1^* x_1 x_2 + \beta_2 x_1 x_3 + \beta_3 x_1 x_7 - (\phi + \mu)x_2,$$

$$(54) \quad \frac{dx_3}{dt} = f_3 = \phi(1 - \sigma)x_2 - (\theta + d_1 + \mu)x_3,$$

$$(55) \quad \frac{dx_4}{dt} = f_4 = b\pi + \phi\sigma x_2 - (\tau + \mu)x_4,$$

$$(56) \quad \frac{dx_5}{dt} = f_5 = \tau\rho x_4 + \theta x_3 - (\alpha + d_2 + \mu)x_5,$$

$$(57) \quad \frac{dx_6}{dt} = f_6 = \tau(1 - \rho)x_4 + \alpha x_5 - \mu x_6,$$

$$(58) \quad \frac{dx_7}{dt} = f_7 = k_1 x_2 + k_2 x_3 - \epsilon x_7.$$

The variational matrix of the model (52)-(58) evaluated at the infection-free equilibrium $\mathcal{D}_0 = \mathbf{x} = (x_1 = S_0, x_2 = 0, x_3 = 0, x_4 = 0, x_5 = 0, x_6 = 0, x_7 = 0)$ is derived thus

$$(59) \quad J^* = J(\mathcal{D}_0)|_{\beta_1 = \beta_1^*} = \begin{pmatrix} -\mu & -\beta_1^* S_0 & -\beta_2 S_0 & 0 & 0 & 0 & -\beta_3 S_0 \\ 0 & -p_1 + \beta_1^* S_0 & \beta_2 S_0 & 0 & 0 & 0 & 0 \\ 0 & \phi(1 - \sigma) & -p_2 & 0 & 0 & 0 & 0 \\ 0 & \phi\sigma & 0 & -p_3 & 0 & 0 & 0 \\ 0 & 0 & \theta & \tau\rho & -p_4 & 0 & 0 \\ 0 & 0 & 0 & \tau(1 - \rho) & \alpha & -\mu & 0 \\ 0 & k_1 & k_2 & 0 & 0 & 0 & -\epsilon \end{pmatrix},$$

where $p_3 = (\tau + \mu)$ and $p_4 = (\alpha + d_2 + \mu)$. Assuming $\beta_1 = \beta_1^*$ denotes the bifurcation parameter and $\mathcal{R}_c = 1$ represents the bifurcation point. Expressing β_1^* the subject of the equation when $\mathcal{R}_c = 1$ in Eq.(30) then

$$(60) \quad \beta_1^* = \frac{\epsilon p_1 p_2 - X S_0}{p_2 \epsilon S_0},$$

where

$$X = \epsilon \beta_2 \phi(1 - \sigma) + k_1 p_2 \beta_3 + k_2 \phi(1 - \sigma).$$

Really, $\beta_1^* = \frac{\beta_1}{\mathcal{R}_c}$ while \mathcal{R}_c is a function of β_1^* . The variational matrix $J^* = J(\mathcal{D}_0)|_{\beta_1 = \beta_1^*}$ consists of a right-eigenvector in terms of zero eigenvalue at $\beta_1 =$

β_1^* denoted by

$$\mathbf{w} = [w_1, w_2, w_3, w_4, w_5, w_6, w_7]^T,$$

such that for $w_2 = w_2 > 0$, there exists

$$(61) \quad w_1 = -\frac{S_0[p_2\beta_1^*\epsilon + \beta_2\phi(1-\sigma)\epsilon + (\beta_3k_1p_2 + \beta_3k_2\phi(1-\sigma))]}{\epsilon p_2}w_2,$$

$$(62) \quad w_2 = w_2 > 0,$$

$$(63) \quad w_3 = \frac{\phi(1-\sigma)}{p_2}w_2 > 0,$$

$$(64) \quad w_4 = \frac{\phi\sigma}{p_3}w_2 > 0,$$

$$(65) \quad w_5 = \frac{p_2\tau\rho\phi\sigma + p_3\theta\phi(1-\sigma)}{p_2p_3p_4}w_2 > 0,$$

$$(66) \quad w_6 = \frac{[p_2p_4\tau\phi\sigma(1-\rho) + p_2\alpha\tau\rho\phi\sigma + p_3\alpha\theta(1-\sigma)]}{\mu p_2p_3p_4}w_2 > 0,$$

$$(67) \quad w_7 = \frac{k_1p_2 + k_2\phi(1-\sigma)}{\epsilon p_2}w_2 > 0.$$

Also, the variational matrix $J^* = J(\mathcal{D}_0)|_{\beta_1=\beta_1^*}$ has a left-eigenvector

$$\mathbf{v} = [v_1, v_2, v_3, v_4, v_5, v_6, v_7]^T,$$

which is related to the zero eigenvalue at $\beta_1 = \beta_1^*$ satisfying the condition $\mathbf{v} \cdot \mathbf{w} = 1$ such that for $v_2 = v_2 > 0$, there exists $v_1 = v_3 = v_4 = v_5 = v_6 = v_7$.

The related nonzero derivatives of \mathbf{f} that exist at the infection-free equilibrium \mathcal{D}_0 are worked out as:

$$(68) \quad \frac{2v_2w_1w_2\partial^2 f_2}{\partial x_1\partial x_2}(0, 0) = 2v_2w_1w_2\beta_1^*,$$

$$(69) \quad \frac{2v_2w_1w_3\partial^2 f_2}{\partial x_1\partial x_3}(0, 0) = 2v_2w_1w_3\beta_2,$$

$$(70) \quad \frac{2v_2w_1w_7\partial^2 f_2}{\partial x_1\partial x_7}(0, 0) = 2v_2w_1w_7\beta_3,$$

$$(71) \quad \frac{v_2w_2\partial^2 f_2}{\partial x_2\partial \beta_1^*}(0, 0) = v_2w_2S_0.$$

Item (iv) Theorem 4.1 in [11] is then used to get the final result having obtained the nonzero derivatives of \mathbf{f} at the infection-free equilibrium \mathcal{D}_0 . Following article (iv), Theorem 4.1 in [11],

$$\begin{aligned} a &= \sum_{k,i,j=1}^7 v_k w_i w_j \frac{\partial^2 f_k}{\partial x_i \partial x_j}(0, 0), \\ &= 2v_2 w_1 [w_2 \beta_1^* + w_3 \beta_2 + w_7 \beta_3]. \end{aligned}$$

Notice that $w_1 < 0$ but $w_2 > 0, w_3 > 0$ and $v_7 > 0$ in Eqs. (61),(62),(63) and (67) respectively. Therefore,

$$(72) \quad a = -2v_2w_1[w_2\beta_1^* + w_3\beta_2 + w_7\beta_3] < 0,$$

and,

$$(73) \quad \begin{aligned} a &= \sum_{k,i=1}^7 v_k w_i \frac{\partial^2 f_k}{\partial x_i \partial \beta_1^*}(0, 0), \\ &= v_2 w_2 S_0. \end{aligned}$$

The analytical results of a and b in Eqs. (72) and (73) show that $a < 0$ and $b > 0$. It then follows from the same article (iv) in Theorem 4.1 [11] that there exists a unique infection-persistence equilibrium in the neighborhood of \mathcal{D}_0 that is locally asymptotically stable whenever $\mathcal{R}_c > 1$ (the condition also imposes $\beta_1^* < \beta_1$). \square

Global Stability Analysis of Nonzero Equilibrium. All along, the stability analysis has been restricted to the neighborhood of \mathcal{D}_0 , the infection-free equilibrium point. If the analysis is extended beyond the neighborhood of \mathcal{D}_0 when $\mathcal{R}_c > 1$ then we can discuss the global stability of the infection-persistence equilibrium.

Theorem 3.3. *The infection-persistence equilibrium \mathcal{D}^* of the COVID-19 model is globally asymptotically stable if $\mathcal{R}_c > 1$ such that the time derivative of the Lyapunov function \mathcal{V} of the system is negative definite, i.e., $\frac{d\mathcal{V}}{dt} < 0$.*

Proof. Since the analysis is outside the neighborhood of \mathcal{D}_0 then the technique of nonlinear Lyapunov function as in [6,9] can be used to investigate the global stability of the infection-persistence equilibrium of the model. We therefore construct the Lyapunov function

$$(74) \quad \begin{aligned} V(S^*, E^*, I^*, Q^*, H^*, R^*, V^*) &= \left(S - S^* - S^* \log \frac{S^*}{S} \right) + \left(E - E^* - E^* \log \frac{E^*}{E} \right) \\ &+ \left(I - I^* - S^* \log \frac{I^*}{I} \right) + \left(Q - Q^* - Q^* \log \frac{Q^*}{Q} \right) \\ &+ \left(H - H^* - H^* \log \frac{H^*}{H} \right) + \left(R - R^* - R^* \log \frac{R^*}{R} \right) \\ &+ \left(V - V^* - V^* \log \frac{V^*}{V} \right). \end{aligned}$$

Direct computation of time derivative of (74) gives

$$(75) \quad \frac{dV}{dt} = \left(1 - \frac{S^*}{S}\right) \frac{dS}{dt} + \left(1 - \frac{E^*}{E}\right) \frac{dE}{dt} + \left(1 - \frac{I^*}{I}\right) \frac{dI}{dt} + \left(1 - \frac{Q^*}{Q}\right) \frac{dQ}{dt} + \left(1 - \frac{H^*}{H}\right) \frac{dH}{dt} + \left(1 - \frac{R^*}{R}\right) \frac{dR}{dt} + \left(1 - \frac{V^*}{V}\right) \frac{dV}{dt}.$$

Appropriate substitution of (1)-(7) into (75) and ample simplification gives

$$(76) \quad \frac{dV}{dt} = Z + Y,$$

where

$$(77) \quad Z = b(1 - \pi) \left(1 - \frac{S^*}{S}\right) + (\beta_1 S E + \beta_2 I S + \beta_3 S V) \left(1 - \frac{E^*}{E}\right) + \phi(1 - \sigma) E \left(1 - \frac{I^*}{I}\right) + (b\pi + \phi\sigma E) \left(1 - \frac{Q^*}{Q}\right) + (\tau\rho Q + \theta I) \left(1 - \frac{H^*}{H}\right) + (\tau(1 - \rho)Q + \alpha H) \left(1 - \frac{R^*}{R}\right) + (k_1 E + k_2 I) \left(1 - \frac{V^*}{V}\right),$$

and,

$$(78) \quad Y = (\beta_1 S^* E + \beta_2 I S^* + \beta_3 S^* V + \mu S^*) \left(1 - \frac{S}{S^*}\right) + p_1 E^* \left(1 - \frac{E}{E^*}\right) + p_2 I^* \left(1 - \frac{I}{I^*}\right) + p_3 Q^* \left(1 - \frac{Q}{Q^*}\right) + p_4 H^* \left(1 - \frac{H}{H^*}\right) + \mu R^* \left(1 - \frac{R}{R^*}\right) + \epsilon V^* \left(1 - \frac{V}{V^*}\right),$$

with $p_1 = \phi + \mu, p_2 = \theta + d_1 + \mu, p_3 = \tau + \mu$ and $p_4 = \alpha + d_2 + \mu$. Since \mathcal{D}^* is a point in \mathcal{D}_0 , i.e., $\mathcal{D}^* \leq \mathcal{D}_0$ then $S^* \leq S, E^* \leq E, I^* \leq I, Q^* \leq Q, H^* \leq H, R^* \leq R$ and $V^* \leq V$. The implication is that Z is positive while Y is negative if $S^* < S, E^* < E, I^* < I, Q^* < Q, H^* < H, R^* < R$ and $V^* < V$. Hence, $\frac{dV}{dt}$ is negative definite, i.e., $\frac{dV}{dt} < 0$ if $Z < Y$. Also, $\frac{dV}{dt} = 0$ if $S^* = S, E^* = E, I^* = I, Q^* = Q, H^* = H, R^* = R$ and $V^* = V$.

Hence, the singleton $\{\mathcal{D}^*\} \in \left\{ (S^*, E^*, I^*, Q^*, H^*, R^*, V^*) \in \Omega : \frac{dV}{dt} = 0 \right\}$ remains the largest compact set, where \mathcal{D}^* is the infection-persistence equilibrium of the model. By LaSalle’s invariance principle in [22], $\frac{dV}{dt} < 0, \mathcal{R}_c > 1$ and the infection-persistence equilibrium \mathcal{D}^* of the model is globally asymptotically stable if $Z < Y$. \square

4. Numerical Experiment and Discussion

Simulation is necessary to justify the theoretical results. A group of numbers that are shown in Table 2, whose sources are from [20,32] as well as assumption,

is used for the model parameters to conduct the simulation. The definitions for the parameters have been stated in Table 1.

TABLE 2. Values for the model parameters.

Parameters	Values	Units
b	125	individual/day
π	0.112	-
β_1	0.035	1/day
β_2	0.082	1/day
β_3	0.011	1/day
μ	0.000037	1/day
ϕ	0.251	1/day
σ	0.012	-
θ	0.154	1/day
d_1	0.017	1/day
d_2	0.013	1/day
τ	0.021	1/day
ρ	1/7	-
α	1/14	1/day
k_1	0.000111	per individual per day
k_2	0.077	per individual per day
ϵ	1	per individual per day per ml

With the values in Table 2, the numerical values for the model equilibria \mathcal{D}_0 and \mathcal{D}^* are computed, where $\mathcal{D}_0 = (S_0, E_0, I_0, Q_0, H_0, R_0, V_0) = (3000000, 0, 0, 0, 0, 0, 0)$ and $\mathcal{D}^* = (S^*, E^*, I^*, Q^*, H^*, R^*, V^*) = \{1, 24, 35, 669, 88, 548760, 2150727493\}$. The numerical results for \mathcal{D}_0 and \mathcal{D}^* indicate that $\mathcal{R}_c > 1$ within the region of parameter space of consideration. The evidence for $\mathcal{R}_c > 1$ is the existence of \mathcal{D}^* and the positivity of all the coordinates of \mathcal{D}^* . As regards the stability of equilibria of the model, the same parameter values in Table 2 are used to evaluate the trace of matrix A ($tr(A)$) and the determinant of matrix A ($det(A)$) in Eq.(33). The quantitative values for $tr(A)$ and $det(A)$ in Eq. (33) are 105 000 and -87 000 respectively. Since $tr(A) > 0$ and $det(A) < 0$, it is straightforward to conclude that the infection-free equilibrium of the model is locally asymptotically unstable. Hence, It follows that $\mathcal{R}_c > 1$ in (51) and there exists a unique infection-persistence equilibrium which has been proved to be locally asymptotically stable in Theorem 4 following the approach in [11].

The interpretation of the results is that COVID-19 is sure to spread should an agent of infection get into the population. The behavior of the ongoing COVID-19 pandemic has been justified by the stability results of the study. To date, there is no place where the virus gets to and fails to spread. Particularly, the virus spread like the harmattan fire in the year 2020. However, the

infectivity and mortality of the pandemic were checked by quarantine and hospitalization during the period. The effect of quarantine and hospitalization on the transmission dynamics of COVID-19 is studied quantitatively by changing the values of quarantine and hospitalization terms (π, σ and θ) and the results are displayed in Figure 2. To plot Figure 2, the initial values for the state variables are taken as $S(0) = 9000, E(0) = 2000, I(0) = 150, Q(0) = 900, H(0) = 100, R(0) = 75, V(0) = 10$ and the values for the parameters except π, σ and θ remain as in Table 2 with the initial human populations measured in thousand and the initial pathogen population in *ml*.

In Figure 2, it is shown that the populations of individuals in the quarantine and hospitalized compartments increase continuously (a and b in Figure 2) as the quarantine and hospitalization terms π, σ and θ increase to 0.611, 0.412 and 0.455 respectively. The populations of individuals in the asymptomatic and symptomatic compartments firstly rise but begin to drop after a month and five months respectively (c and d in Figure 2). The falling parts of curves c and d in Figure 2 are due to the continuous rising of curves a and b in Figure 2.

As more and more asymptomatic and symptomatic individuals are quarantined and hospitalized respectively (a and b in Figure 2), the populations of the asymptomatic and symptomatic individuals diminish (falling parts of c and d in Figure 2). Also, a continuous increase in hospitalization (b in Figure 2) increases the population of the recovered individuals continuously (e in Figure 2). The results in Figure 2 have captured the behavior of the ongoing COVID-19 pandemic perfectly especially during the toughest period in 2020. The population of individuals who were asymptotically and symptomatically infected in the epicenters (China, Italy and the US) firstly rises but begins to fall (rising and falling parts of c and d in Figure 2) and the countries were able to overcome imminent destruction posed by the pandemic at onset with adequate quarantine of exposed individuals as well as individuals who arrive from other countries and hospitalization of infectious individuals (a and b in Figure 2) as the population of the recovered individuals increases continuously (e in Figure 2).

5. Conclusion

In this work, the impact of quarantine and hospitalization on the improved recovery and reduction in the populations of both asymptomatic and symptomatic infectious individuals in the ongoing COVID-19 pandemic particularly during the toughest period of the pandemic in 2020 had been assessed via a deterministic model of a system of first-order nonlinear ordinary differential equations. The basic properties of the model in terms of existence, positivity and boundedness of solutions were proved and the model was then studied qualitatively. The control reproductive ratio was obtained and applied to study the

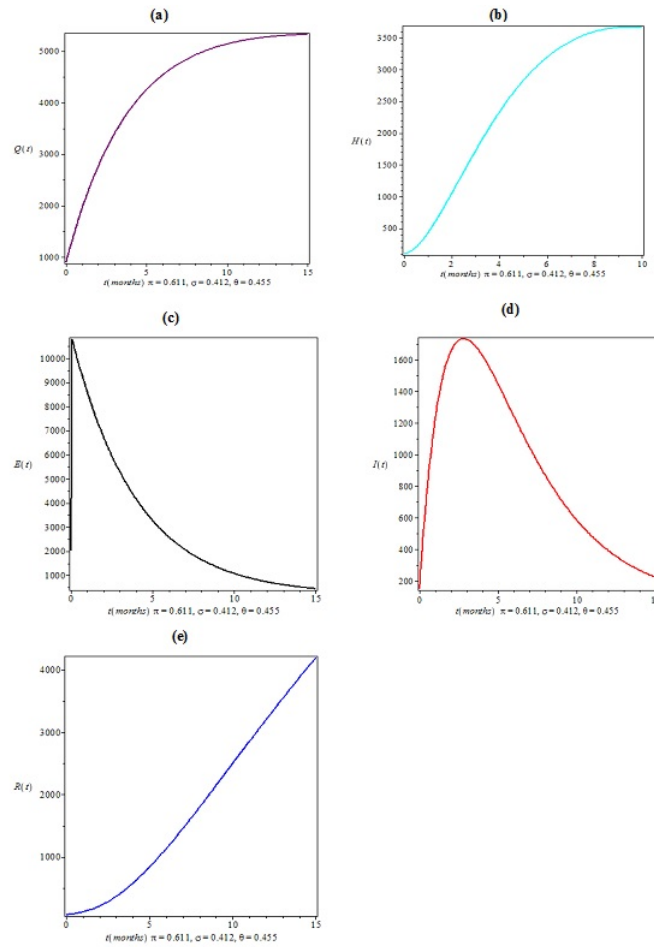


FIGURE 2. A simulation showing the effect of increase in the value of the quarantine and hospitalization terms on the populations of quarantine, hospitalized, asymptomatic, symptomatic and recovered individuals.

local and global stability of the infection-free and infection-persistence equilibria. The conditions necessary and sufficient for both equilibria to be locally and globally asymptotically stable were derived in terms of the control reproductive ratio. Numerical experiment was performed and it was shown that while the infection-free equilibrium of the model was locally and globally asymptotically unstable, the infection-persistence equilibrium of the model was locally and globally asymptotically stable. It was also shown from the simulation that

the adoption and enhancement of quarantine and hospitalization strategies reduced the populations of both asymptomatic and symptomatic individuals but increased the population of the recovered individuals. The downward slopes towards zero of the populations of both the asymptomatic and symptomatic infectious individuals in the simulation revealed that quarantine and hospitalization strategies restore the hope of championing the ongoing COVID-19 pandemic particularly during the toughest period of the outbreak in 2020.

6. Acknowledgement

We would like to thank the reviewers for their thoughtful comments and efforts towards improving our manuscript.

References

- [1] A. Al-Arjani, M.T. Nasseef, S.M. Karmal, . . . , M.S. Uddin, *Application of mathematical modeling to prediction of COVID-19 transmission dynamics*, Arab J. Sci. Eng. **17** (2022), <https://doi.org/10.1007/s13369-021-06419-4>
- [2] N. Al-Asuoad, S. Alaswad, L. Rong, M. Shillor, *Mathematical model and simulations of MERS outbreak: Predictions and implications for control measures*, Biomath. **5** (2017), Article ID 1612141. <http://dx.doi.org/10.11145/j.biomath.2016.12.141>
- [3] J. A. Addor, A. J. Turkson, D. Y. Kparib, *A mathematical model for the growth dynamics of demand in the fashion industry within the era of the COVID-19 Pandemic*, International Journal of Mathematics and Mathematical Sciences Volume 2022, Article ID 5873432, <https://doi.org/10.1155/2022/5873432>
- [4] A.A. Ayoade, O.J. Peter, T.A. Ayoola, S. Amadiogwu, A.A. Victor, *A saturated treatment model for the transmission dynamics of rabies*, Malaysian J. of Computing, **4** (1) (2019), 201-213.
- [5] A.A. Ayoade, M.O. Ibrahim, O.J. Peter, F.O. Oguntolu, *A mathematical model on cholera dynamics with prevention and control*, Covenant J. of Physical & Life Sci.(CJPL), **6**(6) (2018), 46-54.
- [6] A.A. Ayoade, M.O. Ibrahim, O.J. Peter, F.A. Oguntolu, *On the global stability of cholera model with prevention and control*, Malaysian J. of Computing, **3** (2018), 28-36.
- [7] A.A. Ayoade, T. Latunde, R.O. Folaranmi, *Comparative analysis of transmissibility and case fatality ratio of SARS, MERS and COVID-19 via a mathematical modeling approach*, J. Fundam. Appl. Sci. **13**(3) (2021), 1262-1274.
- [8] A.A. Ayoade, O. Aliu, *COVID-19 outbreak and mitigation by movement restrictions: a mathematical assessment of economic impact on Nigerian households*, Journal of Quality Measurement and Analysis, **18**(2) (2022), 29-44.
- [9] A.A. Ayoade, M.O. Ibrahim, *Analysis of transmission dynamics and mitigation success of COVID-19 in Nigeria: An insight from a mathematical model*, The Aligarh Bulletin of Mathematics, **41**(1) (2022), 1-26.
- [10] F. Bilgili, M. Dundar, S. Kus, kaya, D.B. Lorente, F. Ünlü, P. Gençoglu, E. Mugaoglu, *The age structure, stringency policy, income, and spread of coronavirus disease 2019: evidence from 209 countries*, Front. Psychol. **11** (2021), Article ID 632192. [doi:10.3389/fpsyg.2020.632192](https://doi.org/10.3389/fpsyg.2020.632192)
- [11] C. Castillo-Chavez, B. Song, *Dynamical models of tuberculosis and their applications*, Math Biosci Eng. **1**(2004), 361-404.
- [12] Centers for Disease Control and Prevention: 2019 novel coronavirus. Available from: <https://www.cdc.gov/coronavirus/2019-ncov>

- [13] N. Chen, M. Zhou, X. Dong, J. Qu, F. Gong, Y. Han *et al.*, *Epidemiological and clinical characteristics of 99 cases of 2019 novel coronavirus pneumonia in Wuhan, China: a descriptive study*, *The Lancet*, (2020) [https://doi.org/10.1016/S0140-6736\(20\)30211-7](https://doi.org/10.1016/S0140-6736(20)30211-7)
- [14] B. Z. Dieudonne, *Mathematical model for the mitigation of the economic effects of the COVID-19 in the Democratic Republic of the Congo*, *PLoS ONE*, **16**(5) (2021), e0250775. <https://doi.org/10.1371/journal.pone.0250775>
- [15] P.V.D. Driessche, J. Watmough, *Reproduction numbers and sub-threshold endemic equilibria for compartmental models of disease transmission*, *Math. Biosci.* **180**(2002) 29-48. [https://doi.org/10.1016/S0025-5564\(02\)00108-6](https://doi.org/10.1016/S0025-5564(02)00108-6)
- [16] T. Ellerin, *The new coronavirus: What we do- and don't- know*, *Harvard Health Blog*. January 25, 2020. Available from: <https://www.health.harvard.edu/blog/the-new-coronavirus-what-we-do-and-dont-know-2020012518747>
- [17] L.E. Gralinski, V.D. Menachery, *Return of the coronavirus: 2019-nCoV*, *Viruses*, **12** (135) (2020), 135-142.
- [18] A.B. Gumel, *Using mathematics to understand and control the 2019 novel coronavirus pandemic*, *This Day Live*, May 3, (2020) Available at <https://www.thisdaylive.com/index.php/2020/05/03/using-mathematics-to-understand-and-control-the-2019-novel-coronavirus-pandemic/> [Accessed December 4, 2021].
- [19] P. Harjule, R.C. Poonia, B. Agrawal, A.K.J. Saudagar, A. Altameem, M. Alkhatami, M.B. Khan, M.H.A. Hasanat, K.M. Malik, *An effective strategy and mathematical model to predict the sustainable evolution of the impact of the pandemic lockdown*, *Healthcare*, **10** (2022), 759. <https://doi.org/10.3390/healthcare10050759>
- [20] E. Iboi, O.O. Sharomi, C. Ngonghala, A.B. Gumel, *Mathematical modeling and analysis of COVID-19 pandemic in Nigeria*, *Math. Biosci. and Eng.* Vol. 17, no. 6, (2020) 7192-7220. doi: 10.3934/mbe.2020369
- [21] N.Imai, A. Cori, I. Dorigatti, M. Baguelin, C.A. Donnelly, S. Riley *et al.* Report 3: transmissibility of 2019-nCoV, (2020) Available from: <https://www.imperial.ac.uk/mrc-global-infectious-disease-analysis/news-wuhan-coronavirus/>.
- [22] J.P. LaSalle, *The stability of dynamical systems*, Regional Conference Series in Applied Mathematics, SIAM, Philadelphia, Pa, (1976).
- [23] Q. Li, X. Guan, P. Wu, X. Wang, L. Zhou, Y. Tong *et al.*, *Early transmission dynamics in Wuhan, China, of novel coronavirus-infected pneumonia*, *N. Engl. J. Med.* Vol. 5 (2020), 21-29.
- [24] R. Lu, X. Zhao, J. Li, P. Niu, B. Yang, H. Wu *et al.*, *Genomic characterization and epidemiology of 2019 novel coronavirus: implications for virus origins and receptor binding*, *The Lancet*, (2020), [https://doi.org/10.1016/S0140-6736\(20\)30251-8](https://doi.org/10.1016/S0140-6736(20)30251-8)
- [25] R.W. Mbogo, J.W. Odhiambo, *COVID-19 outbreak, social distancing and mass testing in Kenya - insight from a mathematical model*, *Afrika Matematika*, Vol. 13, (2021) 1-6.
- [26] A. Patel, D. Jernigan, nCoV CDC response team: initial public health response and interim clinical guidance for the 2019 novel coronavirus outbreak- United States, December 31, 2019- February 4, 2020. *MMWR Morb Mortal Wkly Rep.* (2020) <https://doi.org/10.15585/mmwr.mm6905e1>
- [27] J.M. Read, J.R.E. Bridgen, D.A.T. Cummings, A. Ho, C.P. Jewell, *Novel coronavirus 2019-nCoV: early estimation of epidemiological parameters and epidemic size estimates*, *Philosophical Transactions of The Royal Society B Biological Sciences*, Vol. 376, no. 1829, (2020) Article ID 20200265 DOI:10.1098/rstb.2020.0265
- [28] C. Rothe, M. Schunk, P. Sothmann, G. Bretzel, G. Froeschl, C. Wallrauch *et al.*, *Transmission of 2019-nCoV infection from an asymptomatic contact in Germany*, *N. Engl. J. Med.* Vol. 5, (2020) 7-12.

- [29] B. Tang, X. Wang, Q. Li, N.L. Bragazzi, S. Tang, Y. Xiao *et al.*, *Estimation of the transmission risk of 2019-nCoV and its implication for public health interventions*, J. Clin. Med. Vol. 9, (2020) 462-469.
- [30] WHO statement regarding cluster of pneumonia cases in Wuhan, China. 2020. Available from: <https://www.who.int/china/news/detail/09-01-2020-who-statement-regarding-cluster-of-pneumonia-cases-in-wuhan-china>, Accessed April 15, 2021.
- [31] J-T. Wu, K. Leung, G.M. Leung, *Nowcasting and forecasting the potential domestic and international spread of the 2019-nCoV outbreak originating in Wuhan, China: a Modeling study*, The Lancet, Vol. 395, (2020) 689-697.
- [32] C. Yang, J. Wang, *A mathematical model for the novel coronavirus epidemic in Wuhan, China*, Maths Biosci. and Eng. Vol. 17, (2020) 2708-2724.
- [33] Z. Yang, Z. Zeng, K. Wang *et al.*, *Modified SEIR and prediction of the epidemics trend of COVID-19 in China under public health interventions*, J. of Thoracic Dis. Vol. 5, (2020) 15-22.
- [34] S. Zhao, Q. Lin, J. Ran, S.S. Musa, G. Yang, W. Wang *et al.*, *Preliminary estimation of the basic reproduction number of novel coronavirus (2019-nCoV) in China, from 2019 to 2020: A data-driven analysis in the early phase of the outbreak*, Int. J. Infect Dis. Vol. 7, (2020) 11-22.
- [35] N. Zhu, D. Zhang, W. Wang, *et al.*, *A novel coronavirus from patients with pneumonia in China*, N. Engl J. of Med. Vol. 382, (2020) 727-733.
- [36] A. Zeb, E. Alzahrani, V.S. Erturk, G. Zaman, *Mathematical model for coronavirus disease 2019 (COVID-19) containing isolation class*, BioMed Research International, (2020) Article ID 3452402, <https://doi.org/10.1155/2020/3452402>
- [37] A. Zeb, A. Atangana, Z.A. Khan, *Deterministic and stochastic analysis of a COVID-19 spread model*, Fractal, Vol. 30, no. 5, (2022), 2240163, DOI: 10.1142/S0218348X22401636

ABAYOMI AYOTUNDE AYOADE

ORCID NUMBER: 0000-0003-3470-0147

DEPARTMENT OF MATHEMATICS

UNIVERSITY OF LAGOS

LAGOS, NIGERIA

Email address: ayoadeabbayomi@gmail.com; ayoayoade@unilag.edu.ng

PASCHAL ANCHOR IKPECHUKWU

ORCID NUMBER: 0000-0001-7364-7719

DEPARTMENT OF MATHEMATICS

UNIVERSITY OF LAGOS

LAGOS, NIGERIA

Email address: ikpechukwupaschal@gmail.com

SRINIVASARAO THOTA

ORCID NUMBER: 0000-0002-3265-5656

DEPARTMENT OF MATHEMATICS, SCHOOL OF SCIENCES

SR UNIVERSITY

WARANGAL, TELANGANA-506371, INDIA

Email address: srinivasarao.thota@sru.edu.in; srinithota@ymail.com

OLUMUYIWA JAMES PETER

ORCID NUMBER: 0000-0001-9448-1164

DEPARTMENT MATHEMATICAL AND COMPUTER SCIENCES

UNIVERSITY OF MEDICAL SCIENCES

ONDO, NIGERIA

Email address: peterjames4real@gmail.com